Specific Beta-Adrenergic Receptor Binding of Carazolol Measured with PET

Marc S. Berridge, A. Dennis Nelson, Lei Zheng, Gregory P. Leisure and Floro Miraldi

Departments of Radiology and Chemistry, Case Western Reserve University School of Medicine and University Hospitals of Cleveland, Cleveland, Ohio

Carazolol is a promising high-affinity beta-adrenergic receptor ligand for the noninvasive determination of beta receptor status using PET. Earlier investigations demonstrated specific receptor binding of carazolol in mice. These PET studies with S(−)-[2″-^{11}C]carazolol in pigs were performed to explore the utility of the tracer for PET receptor studies. **Methods:** Tracer uptake in the heart and lung was measured by PET as a function of time. Receptors were blocked with propranolol and different doses of ICI 118,551 to estimate specific binding. Fluorine-18-1″-Fluorocarazolol and the less active R-enantiomer of [^{11}C]-carazolol were also studied. **Results:** Specific receptor binding was 75% of the total uptake in the heart, preventable and displaceable by propranolol. Dose-dependent competition showed that carazolol binds in vivo to β_1 and to β_2 subtypes. Uptake of the labeled R(+) enantiomer of carazolol was not receptor-specific. **Conclusions:** Carazolol labeled with ^{11}C or ^{18}F is a strong candidate for use in receptor estimation with PET. The in vivo observations were consistent with its known high affinity and slow receptor dissociation rate. Its high specific receptor uptake and low metabolism allow existing kinetic models to be applied for receptor measurements. The ^{11}C label is convenient for repeated administrations, though ^{18}F allowed the long observation periods necessary for measurement of the receptor dissociation rate. If needed, nonspecific uptake can be estimated without pharmacologic intervention by using the labeled R enantiomer.

Key Words: PET; beta-adrenoceptors; heart; carazolol

J Nucl Med 1994; 35:1665–1676

Beta-adrenergic receptors have been implicated in a variety of diseases affecting the heart and brain. The number of receptors in the heart, brain and lymphocytes have been found to be altered by pathological and physiological conditions and by the action of hormones and drugs (*1–6*). Changes in receptor concentration in turn produce a variation in overall tissue response to catecholamines. The assessment of receptor concentration is therefore of interest in the investigation of disease etiology and progression and possibly in diagnosis and treatment. Encouraging results have been obtained by probing the adrenergic system presynaptically with radioiodinated *m*-iodobenzylguanidine (MIBG) (*7–9*). These studies have indicated that useful clinical information can come from measurements of the adrenergic system. However, presynaptic activity is only half of the receptor system, and the availability of information about the presynaptic status serves as further incentive to develop a way to measure the receptors.

Several ligands have been labeled in attempts to measure beta-adrenergic receptors in vivo. Propranolol (*10*), practolol (*11*) and pindolol (*12*) were labeled with ^{11}C for PET use but had kinetic parameters in vivo which were unsuitable for the purpose. Iodopindolol and iodocyanopindolol (*13–17*) have been labeled with radioiodine and have been useful ligands in vitro. Several additional ligands including carazolol were investigated using tritium labels (*18*) with encouraging results. Recently, another high-affinity beta antagonist, CGP 12,177 (*19,20*) has been introduced for PET and has been demonstrated to have measurable specific binding in vivo. It proved the value of a good beta receptor imaging agent, though its hydrophilicity led to low brain uptake (*21*), and it was rapidly metabolized to a degree which caused difficulties for receptor measurement (*19*). A correlation of the physical properties of these beta-adrenergic antagonists with their properties as in vivo imaging agents led us to conclude that a higher affinity ligand is required for the beta-adrenergic system than for other well researched receptor systems. It is also becoming more important for a proposed ligand to cross the blood-brain barrier because of rapidly growing interest in the brain's beta-adrenergic system (*4–6*).

We therefore chose to label carazolol, a high affinity beta antagonist which is relatively subtype nonspecific, with ^{11}C (*22*) and with ^{18}F (*23*). Our preliminary studies showed that labeled carazolol binds specifically in a displaceable and chirality-sensitive fashion to beta-adrenergic receptors in mouse tissues in vivo. They also indicated that carazolol should give satisfactory results in PET imaging. We have therefore carried out PET studies with pigs to determine the uptake and imaging characteristics of carazolol in the

Received Oct. 20, 1993; revision accepted Jan. 13, 1994.

For correspondence or reprints contact: Marc S. Berridge, PhD, Division of Nuclear Radiology, University Hospitals of Cleveland, 2074 Abington Rd., Cleveland, OH 44106.

heart and lung, the specific receptor binding, and the effective receptor subtype specificity during PET studies.

MATERIALS AND METHODS

Pet Scanning

Young pigs weighing approximately 20–35 kg were obtained locally and housed in the university's animal facility. They were anesthetized with sodium pentobarbital and intubated as a precaution against the possibility of respiratory failure. Two 20-gauge catheters were placed in ear veins for tracer and anesthesia administration during the study. The pigs were kept anesthetized throughout all procedures with incremental administrations of pentobarbital as required. A femoral artery was exposed surgically through which a 5-Fr. Cooks pigtail catheter was placed into the descending aorta within 15 cm of the heart and verified by fluoroscopy. A continuous drip of a solution of heparin (10 U/ml) in sterile physiological saline solution was maintained through all catheters, except during injections and blood sampling.

Scans were performed on a modified PETT Electronics/Scanditronix Superpett 3000 (St. Louis, MO), a time of flight (BaF) scanner with four rings of detectors producing seven tomographic slices. The instrument has an experimentally determined in-plane resolution of 4.8 mm and axial resolution of 11.5 mm in the low-resolution mode used for this study. Modifications to the scanner included installation of energy discriminators for each detector crystal, an improved time-of-flight resolution filter, the addition of total randoms and continuous dead time corrections and improved reconstruction software. The reconstruction filters had an in-plane resolution of 12 mm. After each subject was positioned in the scanner with the heart in the center of the scanning zone, a 30-min attenuation measurement was performed using a 3-mCi rotating $^{68}Ge/^{68}Ga$ source.

Tracers were prepared from synthesized starting materials as previously described (*22–24*). Des-isopropyl carazolol (R or S purified enantiomer, as desired) was reductively alkylated with [^{11}C]acetone and with [^{18}F]fluoroacetone to produce [^{11}C]carazolol and [^{18}F]fluorocarazolol, respectively, in >95% enantiomeric purity. The specific activity of labeled carazolol was 2000–6000 Ci/mmole (both radionuclides) and was measured at the time of each injection. Labeled S-carazolol (^{11}C, 2–6 mCi, 1.5 nmole; ^{18}F, 0.5–1.3 mCi, 0.5 nmole) was injected into an ear vein. List mode data collection was begun at the time of injection and continued for 60 min (^{11}C) or 3 hr (^{18}F). The 2–5-ml bolus injection of radiotracer was followed by an immediate 10-ml bolus of normal saline solution to ensure a complete injection. The injection syringe was assayed for radioactivity before and after each injection and the assays were corrected for decay to the time of injection to calculate the administered dose.

During the first 6 min of the scan, blood was withdrawn through a calibrated radioactivity detector (*25,26*) at 5 ml/min using a Harvard pump to give an accurate, finely sampled (10 points/sec) arterial input curve after deconvolution of the raw data. Blood samples were withdrawn thereafter at 5-min and 10-min intervals throughout the scan for blood radioactivity content measurement and analysis of metabolites. At the end of the first data collection, the first pharmacological intervention (intravenous injection of propranolol 3 mg or ICI 118,551 4–30 mg) was performed. Thirty minutes after the drug administration, a second scan was begun, following the same procedure as the first. The second scan used a second injection of high-specific activity tracer which was produced with a second complete cyclotron irradiation and synthesis. There were two variations on the study protocol. A first scan of the less physiologically active R enantiomer of carazolol was followed in the same animal without pharmacological intervention by a scan of the labeled S enantiomer (prepared separately); or a dose of propranolol was injected at 15 min into the scan in order to observe displacement of tracer from the receptors. In some experiments as appropriate, at the end of the second data acquisition a second pharmacological intervention (complete receptor blockade following the partial block with ICI 118,551 or propranolol during the second scan) was performed followed by a third injection of freshly synthesized tracer and a third data acquisition. The three syntheses and scans were performed at 1.5 hr intervals with ^{11}C and at 3.5 hr intervals with ^{18}F. After the final carazolol scan, a perfusion scan was performed. Data was collected from 5 to 15 min after injection of 10 mCi of $^{13}NH_3$ for independent delineation of the myocardium. At the end of the experiment, the pigs were euthanized according to current national and institutional animal research policies.

Data Analysis

The list mode data from the first 10 min of each scan were reconstructed into ten tomographic image sets, each representing 1 min of collected data. Additional image sets were reconstructed from 5-min intervals beginning at 10 min and continuing to the end of the study. During data reconstruction, the total system count rate in 1-sec intervals was routinely used to calculate and apply dead time corrections for each time interval using a paralyzable method (*27*), though the count rates from these studies were such that the dead time correction was small. The dead time parameter (τ) was previously determined from phantom studies to be 1.41 μsecs for our system. The images were corrected for random counts using the time of flight (TOF) characteristics of the camera. Random events were assumed to be uniformly distributed across the imaging field prior to the attenuation correction. Events detected in pixels at the periphery of the imaging field at least 16 cm from the subject were measured. The average number of random events per pixel was then adjusted by the attenuation correction factors for each image pixel and subtracted from the image data. This technique is valid since our TOF resolution is less than 16 cm FWHM (8 cm radially), and has been validated using phantom studies in which PET data was acquired continuously during decay. In the resulting images, the corrected count total per pixel was converted into units of $\mu Ci/cm^3$ using the camera calibration data.

For each study, the images acquired between 30 and 60 min after injection were summed to produce one high-count high-contrast image on which regions of interest (ROIs) representing myocardium, lung and the ventricular cavity were easily defined. The ROIs were well within, and centered on, their respective areas in order to avoid strong partial volume effects. The positioning of the ROIs was checked using the outline of the myocardium given by the [^{13}N]ammonia scans. Other than these precautions, there was no attempt to make corrections for partial volume error. The ROIs were then applied to the entire sequence of images to generate quantitative time-activity curves for each region during each study. The resultant curves were corrected for the radioactive decay of the label, and the scale was normalized by dividing by the injected dose. In sequential studies, a correction was made for the small residual activity in each tissue which remained from the previous injection. The radioactivity which was observed in each region at the end of the previous data acquisition was decay corrected to the beginning of the following

scan. That value was then subtracted from the decay-corrected curve of the following scan, before normalization for injected dose. Though this technique resulted in a small overcorrection due to the slow decline in the residual activity curve, the error was small relative to the magnitude of the correction, which in turn was small with respect to the corrected data.

Metabolite Analysis

For each analysis, 0.5 ml of blood was added to 0.5 ml of ethanol. The mixture was vortex mixed and ultrasonicated for 5 min. It was then centrifuged in an Eppendorf (model 5414, 16,000 × g, Hamburg, Germany) benchtop centrifuge for 7 min and the supernatant collected and added to 9 ml water. The water solution was passed through a Millipore C-18 Sep-pak, which retained unchanged carazolol. The Sep-pak was washed with 2 × 10 ml of water to remove metabolites, and the centrifuged pellet, Sep-pak and washes were assayed for radioactivity. Control experiments were performed by adding labeled carazolol to fresh blood and immediately beginning the procedure in order to measure carazolol breakthrough into the wash fractions. Also as a control experiment, several mCi were injected into a mouse in order to obtain a blood sample which contained metabolites and sufficient radioactivity (injected dose: 100 mCi/kg versus 100 μCi/kg in the pig) for HPLC analysis. The mouse was killed 20 min after tail vein injection and 1.5 ml of blood was withdrawn from the heart. HPLC was performed on the wash fractions, on the Sep-pak retained fraction after elution with ethanol, and on ethanol extracts of the centrifuged pellet. An analytical silica column was used (Alltech Econosil 10 μm, 4.6 × 250 mm, Deerfield, IL) and eluted at 2 ml/min with chloroform containing 2% (v/v) of a solution of 2% methyl amine and 2% water in ethanol (RT: carazolol, 7 min; labeled metabolites, 1–3 min). HPLC results for each fraction were expressed as the percentage of the HPLC-injected sample radioactivity which was recovered in the carazolol fractions; any remainder, the vast majority of which was observed in the metabolite fractions, was assumed to be metabolized.

RESULTS

PET images of labeled carazolol in untreated pigs were of good quality and contrast (Fig. 1). The heart and lungs were clearly seen and were easily distinguishable from each other in the images. An injected dose of 3 mCi was satisfactory for routine studies. Administration of propranolol (3 mg i.v.) before the tracer injection resulted in a much lower uptake of carazolol. Figure 1 represents 1 hr of data gathered from each of two injections (5.2 and 5.3 mCi) in a single pig administered 90 min apart. The second injection was performed after propranolol administration, and both images are scaled to the same quantitative gray scale. Total image counts for the propranolol-blocked scan were only 19% of the total image counts of the untreated scan for this animal.

This qualitative result is quantified and shown as time-activity curves in Figures 2 and 3. The figures show radioactivity content in the heart and lung, respectively, and are decay corrected to the time of injection. The R-carazolol curves represent a single animal. The S-carazolol curves represent an average of six control studies in which scans were acquired with no intervention and three studies after

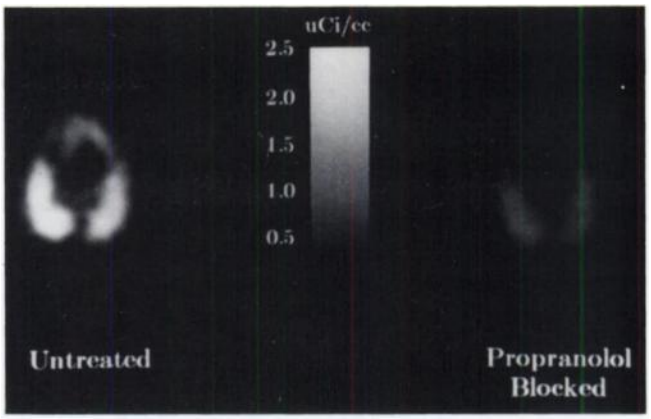

FIGURE 1. Transaxial PET images of a single pig after injection of 5.2 mCi of [^{11}C]S(−)-carazolol (left image) and after a second (5.3 mCi) radiotracer injection after a 3-mg intravenous injection of propranolol (right image). The animal is on its back, the left side to the right of the image. The lungs are seen in each image. The heart is visible as a crescent in the upper portion of the left image. Both images were quantified in units of μCi/cc and are displayed on the same gray scale, as shown.

full receptor blocking (3 mg propranolol in addition to any other blocking dose). The variation between curves from different studies, normalized by injected dose, was less than 7%. Heart and lung uptake was rapid and twice as great in the lung as in the heart. Tracer washout from the tissue after the initial bolus was slow. Blood radioactivity content dropped rapidly in the first 3 min to 0.02–0.04 μCi/ml per injected mCi and remained near this range (decay corrected) throughout the study (Fig. 2). The heart-to-blood activity ratio was 5:7 throughout the study. The uptake of [^{11}C]R(+)-carazolol, the less active enantiomer, is shown in Figures 2 and 3 for comparison with the S(−) enantiomer after propranolol blocking. Propranolol prevented the majority of the binding, as did use of the inactive enantiomer. Propranolol administration did not alter the uptake of R(+)-carazolol (data not shown).

In Figures 2 and 3 the difference between the total binding (solid symbols) and the nonspecific uptake (open symbols) represents the specific receptor binding. This difference as a function of time is shown in Figure 4. The specific binding is shown two ways, using propranolol blocking of S-carazolol binding or the uptake of the R enantiomer of carazolol as the reference for nonspecific uptake. In the heart the two are similar, however, specific binding in the lung appears significantly higher when nonspecific uptake is measured using the R enantiomer.

Another measure of binding which is important for imaging is the ratio of specific binding to nonspecific uptake. This ratio is shown in Figure 5. Figures 2, 4 and 5 show that the noticeable increase in the specific binding ratio in the heart is due to a decline in nonspecific uptake while total uptake increased. In the lung, the total binding decreased throughout the study, so the specific binding ratio was nearly constant after 20 min. Though the total tracer content of the lung is at least twice that of the heart,

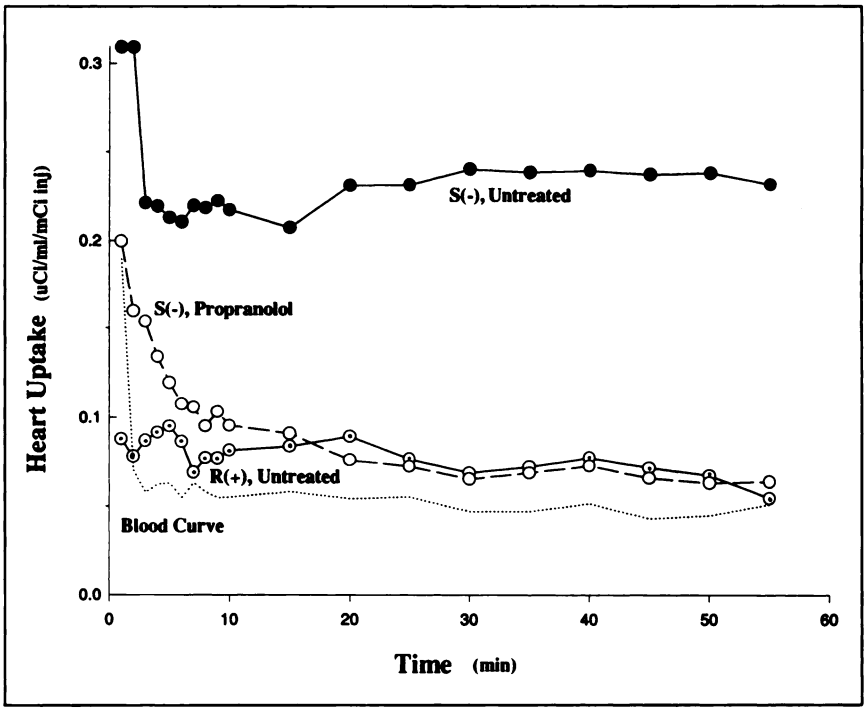

FIGURE 2. Average uptake curves obtained from ROIs over the myocardium after injection of [^{11}C]S(−)-carazolol in untreated animals (solid circles, 5 animals, 6 curves averaged), [^{11}C]S(−)-carazolol after intravenous administration of 3 mg of propranolol (open circles, dashed line, 3 animals, 3 curves averaged), and [^{11}C]R(+)-carazolol in an untreated animal (open dotted circles, solid line, n = 1). Curves are normalized by injected dose. The average blood curve (n = 6) is shown in the same units (dotted line).

the lower nonspecific uptake in the heart gave a specific binding ratio near 4, twice that observed in the lung.

The results of the displacement experiment are shown in Figure 6. Propranolol (3 mg) was injected 15 min after the second tracer injection of the study in a single animal. For comparison, the curves from the untreated experiment are shown in solid symbols and the set of curves for each organ were normalized to approximately the same maximum. The effect of propranolol injection is easily noted from both curves. The untreated heart curve increased, while the displacement curve decreased from the time of propranolol injection. The lung curve normally decreased slightly, but a significant change due to the propranolol injection was clear. The slopes of the two displacement curves were similar. Half-times for ligand displacement estimated from these curves were 250 min in the heart and 125 min in the lung.

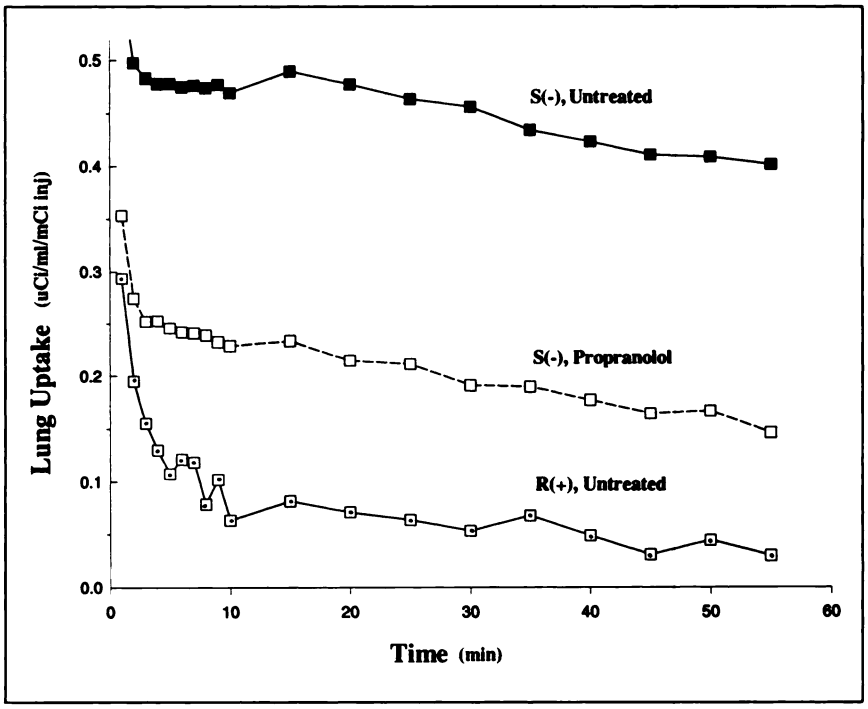

FIGURE 3. Average uptake curves obtained from ROIs over the lung after injection of [^{11}C]S(−)-carazolol in untreated animals (solid squares), [^{11}C]S(−)-carazolol after intravenous administration of 3 mg of propranolol (open squares, dashed line), and [^{11}C]R(+)-carazolol without treatment (open dotted squares, solid line). See Figure 2 for number of observations.

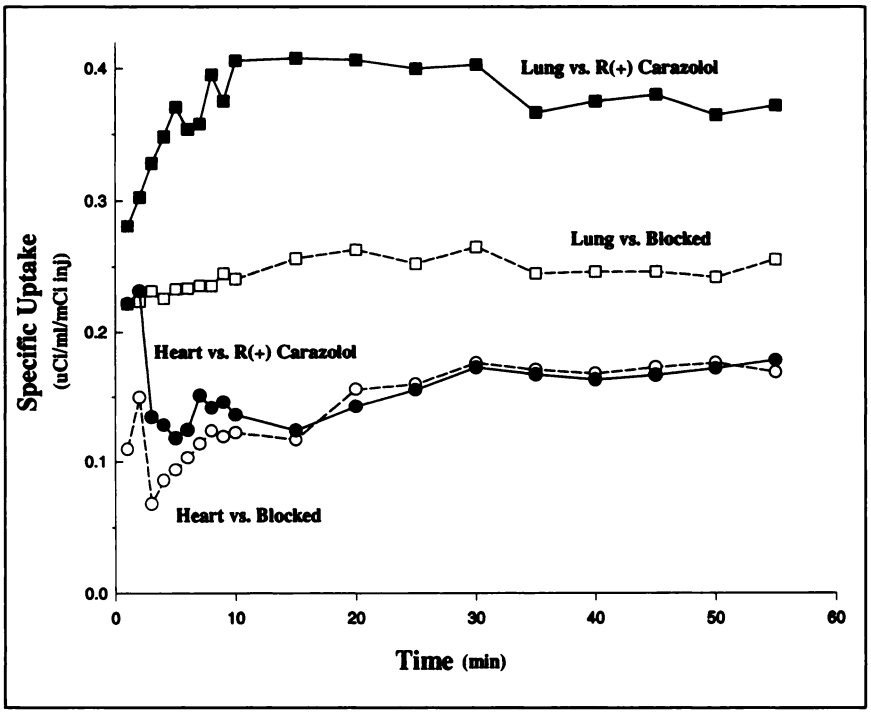

FIGURE 4. Specific uptake (Total – nonspecific uptake, from Figs. 2 and 3) in heart (circles) and lung (squares) as a function of time. Solid symbols represent specific uptake using R-carazolol as the nonspecific reference, open symbols with dashed lines represent specific uptake using S-carazolol after 3 mg of propranolol (i.v.) as the nonspecific reference.

Figures 7 and 8 show the results of administration of 4 and 30 mg of ICI 118,551, a β_2-specific antagonist, in the heart and in the lung, respectively. The effect of increasing dose is apparent in both figures. In the lung the blocking effect is stronger than in the heart. The experiments were performed using two pigs. Each pig received three doses of [^{11}C]carazolol. The first scan was performed as a baseline with no intervention. The second was performed after intravenous injection of 4 or 30 mg of ICI 118,551. The third scan was performed after injection of 3 mg of propranolol to establish the nonspecific uptake for each pig. As was true throughout these studies (Figs. 2 and 3), the curves from each animal were the same within experimental error in the untreated and fully blocked cases. The data is therefore shown in terms of total uptake on a single graph without the need to convert it to percentage of specific binding for each animal.

Results obtained with [^{18}F]fluorocarazolol are shown in

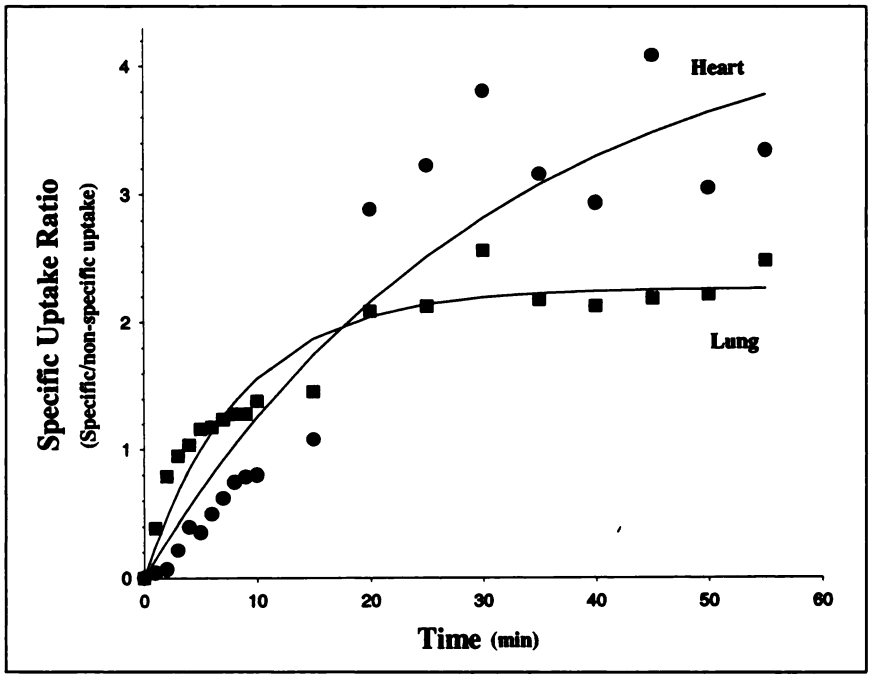

FIGURE 5. Specific-to-nonspecific uptake ratio in heart (circles) and lung (squares) measured as [(total uptake – nonspecific uptake)/(nonspecific uptake)]. See Figure 4 for specific uptake curves.

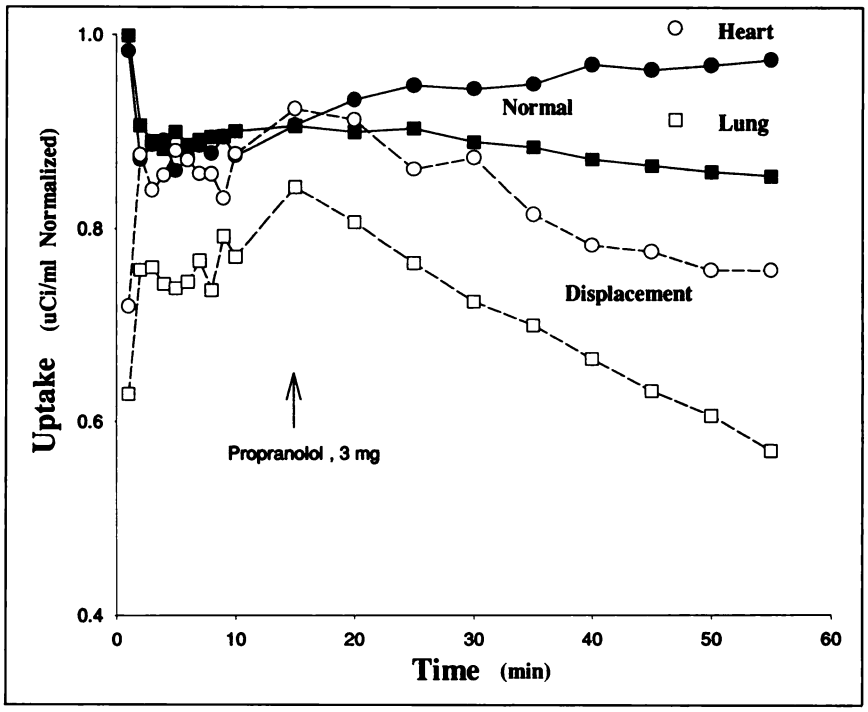

FIGURE 6. Displacement of [^{11}C]S(−)-carazolol from heart (circles) and lung (squares). Solid symbols represent a single untreated control animal, open symbols represent the displacement by injection of propranolol (3 mg) 15 min after the second tracer injection in the same animal. The set of heart curves have been normalized to approximate the lung uptake at 10 min for better comparison, but the displacement curves have not been adjusted relative to their respective control curves.

Figures 9 (uptake curves) and 10 (specific uptake). Uptake in the blood, heart and lung during the first hour was the same as [^{11}C]carazolol. The nonspecific uptake in the lung became equal to that in the heart at 90 min into the study, at a value of 0.02 μCi/ml per injected mCi, decay corrected. The specific receptor uptake curves for heart and lung are shown in Figure 10. The magnitude of the uptake in this experiment was less than that obtained from [^{11}C]carazolol, but the shapes of the curves and their relationship to each other did not change. The decline in specific uptake with time noted in these curves was not evident on the shorter time scale of the ^{11}C study. The half-times for the washout process estimated from these curves were 140 min in the lung and 250 min in the heart. The specific uptake ratio of [^{18}F]fluorocarazolol was similar to that for [^{11}C]carazolol (Fig. 5) and is therefore not shown.

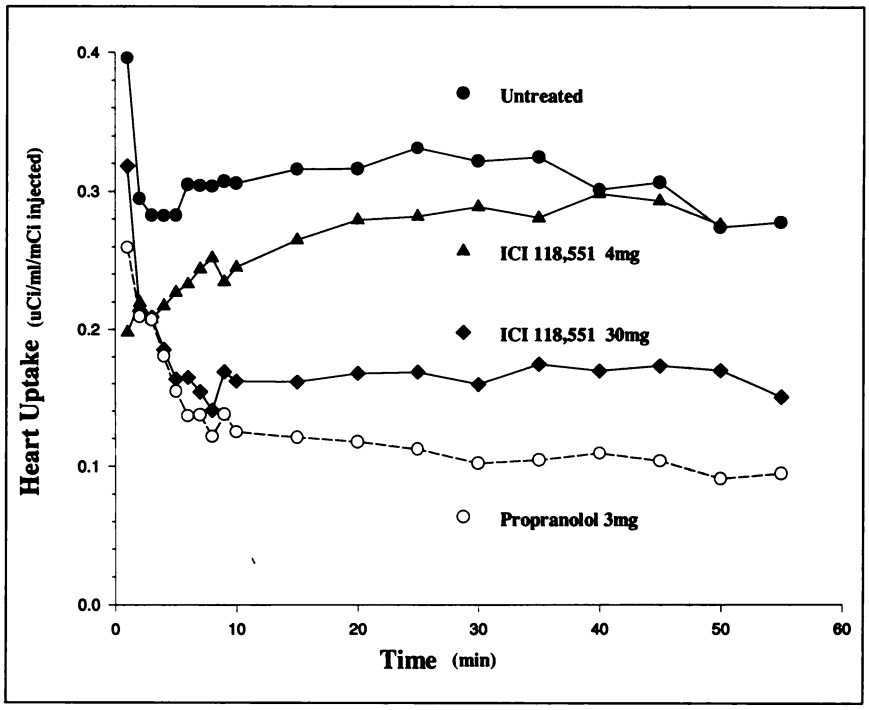

FIGURE 7. Displacement of [^{11}C]S(−)-carazolol from heart by the specific β_2 antagonist ICI 118,551. Curves are shown for untreated control (solid circles), 4-mg dose of ICI 118,551 (solid triangles), 30-mg dose of ICI 118,551 (solid diamonds) and 3-mg dose of propranolol (open circles, dashed line). Data were obtained in two animals from three separate tracer injections each (control, one dose of ICI and propranolol) at 1.5-hr intervals. Control and propranolol curves were not significantly different and were averaged.

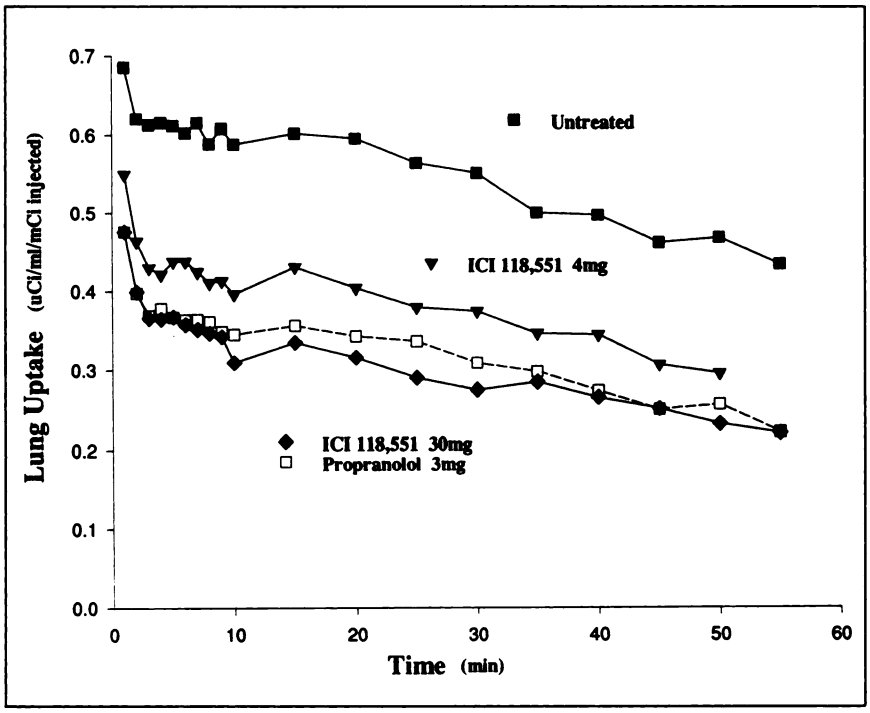

FIGURE 8. Displacement of [^{11}C]S(−)-carazolol from lung by the specific β_2 antagonist ICI 118,551. Curves are shown for untreated control (solid squares), 4-mg dose of ICI 118,551 (solid triangles), 30-mg dose of ICI 118,551 (solid diamonds) and 3-mg dose of propranolol administered for the third study 1.5 hr after 30 mg of ICI 118,551 (open squares, dashed line).

The specific uptake ratios for heart and lung at 1 hr were 4.5 and 3.4, respectively. The ratio in both organs continued to rise slowly, reaching a value of 10 by 150 min. The apparent limit to the uptake ratio which was observed for [^{11}C]carazolol in the lung was not evident in the ^{18}F experiment.

The metabolites in the blood were also examined (Fig. 11). The earliest observation was at 6 min due to the details of blood collection. At that time, metabolites of [^{11}C]-carazolol accounted for 20% ± 2.6% of the activity in the blood. Carazolol comprised 80% ± 5% of the whole-blood activity and was divided evenly between plasma and precipitated solids. Metabolites were negligible in the precipitated pellet. At 6 min, carazolol in the plasma was 42% ± 3% of the total blood activity and 72% ± 4% of the activity in plasma. At times up to 1 hr, these percentages did not

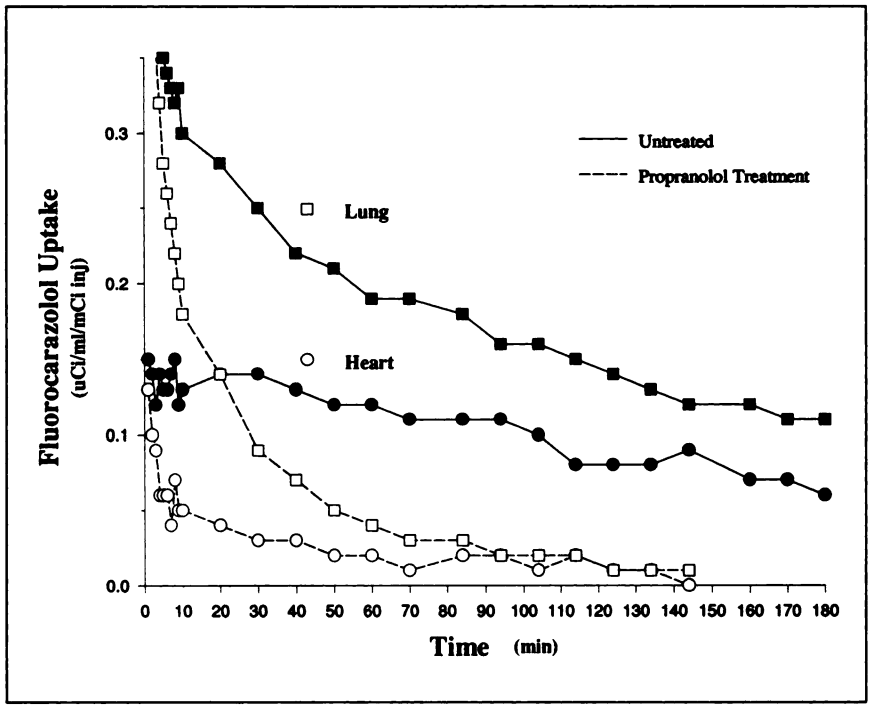

FIGURE 9. Uptake in lung (squares) and heart (circles) of [^{18}F]S(−)-2″-fluorocarazolol in a single animal. Similar to Figures 2 and 3, solid symbols indicate uptake in the untreated animal and open symbols indicate uptake after propranolol treatment.

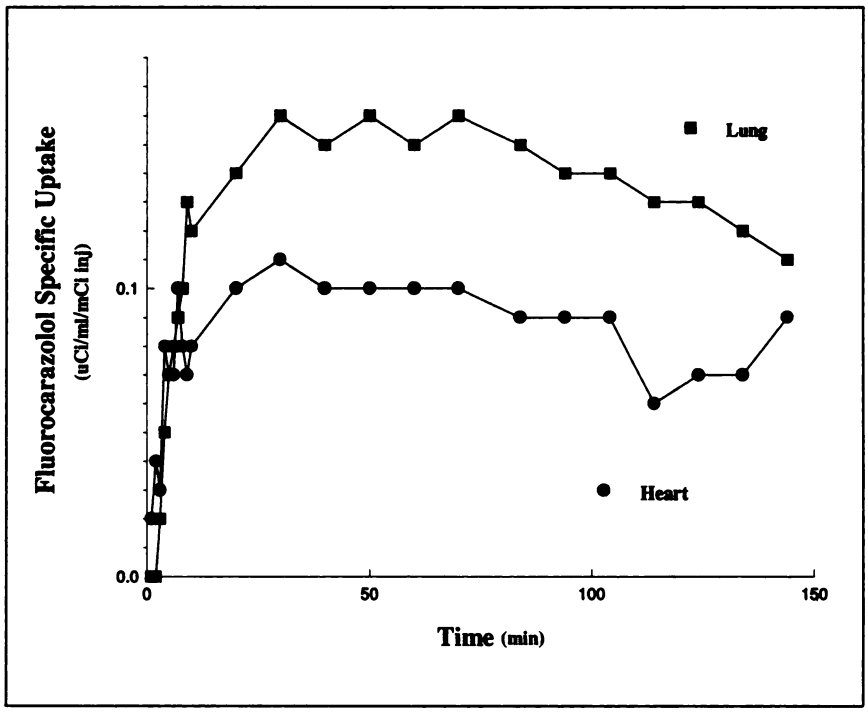

FIGURE 10. Specific uptake in lung (squares) and heart (circles) of [^{18}F]S(−)-2″-fluorocarazolol. Specific uptake was measured after intravenous injection of 3 mg of propranolol as the nonspecific uptake reference (see Fig. 4).

change substantially. Metabolites in the blood decreased smoothly to 13% ± 2% at 1 hr, and the plasma's carazolol content rose to 78% ± 5%. The distribution of [^{11}C]carazolol between plasma and pellet remained constant with 52% ± 2% of the carazolol in the plasma (average and s.d. of all time points, all three [^{11}C]carazolol experiments). The constant division of blood activity between carazolol and metabolites obviously does not reflect on metabolic rate or total body content, but implies that a steady state balance was achieved between production and entry of metabolites into the blood and their removal from the blood. Fluorine-18-labeled fluorocarazolol in a single experiment gave a similar result, except that fluorocarazolol in the pellets comprised only 11% ± 6% of the total activity, as seen in Figure 11 as a higher level of unmetabolized material in plasma. Defluorination was an additional metabolic route for fluorocarazolol which increased at later time points (up to 16% F^-), but again, the distribution of

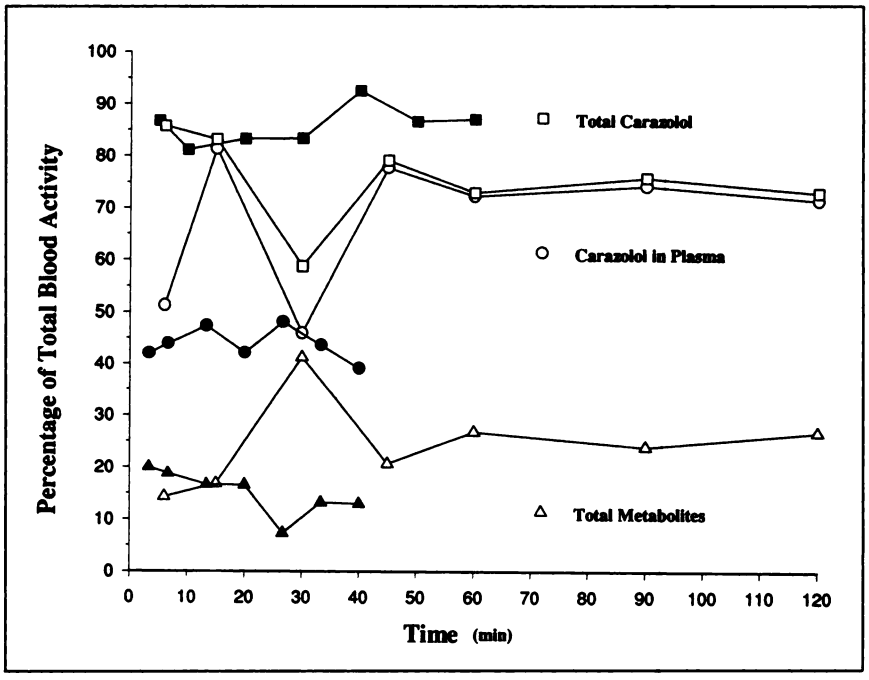

FIGURE 11. Percentage radioactivity in blood representing metabolites and unmetabolized [^{11}C]S(−)-carazolol (solid symbols, n = 3) and [^{18}F]S(−)-2″-fluorocarazolol (open symbols, n = 1). Total metabolite radioactivity (triangles), total unmetabolized radioactivity (squares), and unmetabolized activity recovered in the plasma (circles) are expressed as a percentage of the total blood radioactivity content.

blood radioactivity remained relatively constant throughout the experiment (3 hr) within experimental errors (Fig. 11).

DISCUSSION

Ligands for PET evaluation of receptors can be divided by their kinetic properties into those which are suited to an "equilibrium" data analysis (*28*), and those which are amenable to compartmental kinetic analysis (*29,30*). Because the equilibrium approach places very narrow constraints on the properties of a ligand, we concentrated our search for ligands on those which would be good prospects for the compartmental analysis approach. We examined the existing in vivo data for propranolol, pindolol and practolol (*10–12*), which were not successful in measuring receptor binding, and for iodocyanopindolol (*15–17*) and iodopindolol (*13,14*) which showed much better binding properties. The comparison of the properties of these ligands and kinetic considerations led us to conclude that the affinity required of a successful ligand for the beta-adrenergic receptor may be higher (K_D < ca. 0.2 n*M*) than that required for other receptors which have been imaged. We therefore chose carazolol (K_D 0.01–0.03 n*M*) as a suitable ligand. The results presented here support that analysis. Carazolol was found to have high specific receptor binding in vivo, uptake curves which are similar to those of other successful receptor imaging ligands and reasonably low nonspecific uptake which cleared from the tissue much more rapidly than specifically bound ligand.

The images (Fig. 1) which were obtained with carazolol are well defined, with good contrast and low blood pool activity (heart-to-blood ratio 5–7). The [^{13}N]ammonia perfusion scans were performed primarily to aid in definition of the myocardium if that became necessary due to similar heart and lung tracer uptake. These scans were not needed, or used except to verify a lack of animal movement because the carazolol image contrast made them unnecessary. The uptake of carazolol radioactivity in the heart due to specific receptor interaction is about 80% of the total at 1 hr (Figs. 2–5). When a ^{18}F label is used, the longer observation period allows this quantity to rise to 90%. The high specific binding compares favorably with other high-affinity ligands commonly used for PET. The specific binding observed in pigs was substantially higher than that in mice (*22*). This was expected because the injected dose of carazolol in the mouse appeared to be significant with respect to the receptor population. In the pig the mass of injected tracer relative to the body weight was tenfold less. In the pig heart, the total uptake represented less than 1 pmole/ml, or less than 10% of the expected concentration of receptors in heart tissue.

The total tracer uptake in the lung was greater than in the heart, as expected. Because of the intravenous injection, all of the injected dose passed first through the lung. Much less of the bolus passed through the coronary arteries. Because the lung contains a high concentration of β_2 receptors, one would expect significant binding to occur. The higher washout rate relative to the heart is surprising. Because of the higher affinity for β_2 receptors, a slower washout from the lung would be expected. Instead, the rate in the lung is about twice that in the heart. The apparent discrepancy can be explained if the k_3 for β_2 receptors is a factor of ten higher than for β_1 receptors ($K_D = k_4/k_3$), or if a large component is from a relatively slow tissue washout, and not from receptor binding. The results with ^{18}F-labeled fluorocarazolol showed that the nonspecific uptake in the lung matched that of the heart at 90 min postinjection. The nonspecific uptake might therefore account for some of the decline in total activity in the lung. This hypothesis can only be tested by further compartmental kinetic analysis of the data, which is beyond the scope of this work.

Several methods for mathematical modeling require an independent estimation of nonspecific tissue uptake. In the brain, nonspecific uptake is often measured in the cerebellum, which is assumed to have no receptors. In the case of a beta-adrenergic ligand in the heart, there is no suitable receptor-poor tissue in the field of view. Further, measuring nonspecific uptake using a blocking dose of antagonist, as we have done during this study, is problematic for human subjects. In large doses the antagonists can be life threatening, so it would not be realistic to propose that blocking doses be given in the course of a routine diagnostic procedure. However, Figure 4 demonstrates that a tracer dose of the biologically inactive enantiomer (R-carazolol) accurately represents the nonspecific uptake in the heart. The curve of R-carazolol in the treated or untreated animal is essentially identical to that of S-carazolol after a blocking dose of propranolol. Further, the curve of S-carazolol in the heart (μCi/cc/mCi injected) postpropranolol was very reproducible in spite of variations in animal size (20–35 kg) and heart rate. It also was not affected by the studies in which a blocking, or partially blocking, dose of ICI 118,551 was given previous to the propranolol dose. Each of these points supports the hypothesis that effective beta receptor blockade was achieved in the heart by the propranolol injection.

In the lung, a higher degree of binding of S (postpropranolol) than R enantiomer was seen. This probably indicates that the 3-mg dose of propranolol did not fully block the lung receptors. There is a small chance that the R enantiomer has also overestimated the nonspecific uptake, because it has an affinity for the receptor in vitro which is only one to two orders of magnitude lower than the affinity of the S enantiomer (*31*). This seems unlikely for three reasons. First, rate constant calculations indicate that the R enantiomer should dissociate from the receptor with a half-time less than 1 min, so specific binding should be indistinguishable from nonspecific uptake. Second, other ligands with similar affinity (*10,11*) have shown very low receptor binding in vivo, and third, the results in the heart do not indicate any observable specific binding. It should, therefore, be possible in routine practice to avoid drug

administrations by using separate injections of each enantiomer to measure the total and nonspecific uptake curves when required.

A related consideration to that of nonspecific uptake is that of the effect of changes in perfusion on the tracer uptake. We were not able to quantify perfusion, and the intent of these studies was to determine whether additional studies are justified, so we cannot address the effect of perfusion directly. However, several observations support the view that perfusion was not the overriding factor. During these studies, initial heart rates were 100 min^{-1} to 140 min^{-1}, which generally declined during the study due to the effects of anesthesia and of the adrenergic antagonists. After propranolol administration, the heart rate typically fell by 10%–30%, to 80–110 min^{-1}. This does not seem to be a sufficient decrease to explain the uptake data, though further studies with paired perfusion measurements are clearly indicated. There were no significant differences among all of the control state curves, or among all fully-blocked curves regardless of the mix of antagonists, even though heart rates varied widely between animals. Further, the displacement (Fig. 6) results cannot be explained by perfusion effects. Also, the uptake of R-carazolol (with or without prior propranolol administration) was the same as the propranolol-blocked uptake of S-carazolol in the heart. This stereospecific uptake dependence argues strongly that we have observed a receptor-binding phenomenon. Lastly, the tissue uptake curves (Figs. 2 and 3) and specific binding curves (Fig. 4) show a lack of very high tracer extraction, a rise in specific binding at early times, and a difference between the effectiveness of receptor blockade in heart and lung, all arguing for a receptor number and not a perfusion interpretation.

The displacement experiments (Fig. 6) demonstrate that the specific binding of the ligand can be reversed by a beta antagonist. This has been considered one of the necessary conditions for a receptor-binding tracer (*32*). In Figure 6, there is a clear deviation from the normal curve at the time of propranolol injection, but the displacement rate is not rapid. Assuming first order kinetics, the half-times for displacement from heart and lung as determined by curve-fitting were 270 min and 125 min, respectively. These half-times are consistent with the known in vitro rate constants and high receptor affinity of carazolol.

Experiments using ICI 118,551 demonstrated that carazolol binding was observed to both β_1 and β_2 subtypes, and also show a dose-dependent receptor blocking effect. Because some previous beta-adrenergic receptor ligands of reasonably high affinity had failed to achieve specific binding, and because carazolol has about a fivefold lower affinity for β_1 than for β_2 receptors, we thought it possible that carazolol binding might disproportionately represent β_2 receptors. This was a serious concern since the receptor of major interest in the heart is β_1. We therefore performed the experiments shown in Figures 7 and 8, using two different doses of the β_2-specific antagonist, ICI 118,551. In the lung (Fig. 8), which contains predominantly (90%) β_2 receptors (*31*), a 4-mg dose was sufficient to block 75% of the specific binding, using the propranolol-blocked curve as reference. After a very high (30 mg) dose, the carazolol uptake was similar to the propranolol curve, indicating full blocking of the lung receptors. In the heart (Fig. 7), which contains predominantly (85%) β_1 receptors (*31*), a 4-mg dose was relatively ineffective. It reduced the initial uptake of carazolol by 20% (as estimated at 20 min) but by 60 min the uptake was equal to the unblocked curve. However, the 30-mg dose blocked approximately 70% of the heart uptake. This is the result which would be expected. A pharmacologic dose (4 mg) of a specific β_2 blocker should prevent a large part of lung binding, and a relatively low percentage of heart binding, consistent with the distribution of receptor subtypes in the tissues. Because subtype specificity is not absolute, however, a very large dose (30 mg) of ICI 118,551 would be expected to block the β_2 receptors and many of the β_1 receptors. The observed carazolol binding curves in both organs (Figs. 7 and 8) therefore indicate that carazolol was binding both subtypes of receptors. Although tissue receptors were not assayed in these experiments, the displacement is consistent with the known normal distribution of receptors in heart and lung, and implies a similar efficiency of carazolol binding to both subtypes as observed by PET.

The metabolism of a radiopharmaceutical affects the ability to apply kinetic models because it alters the apparent radiotracer concentration when total blood radioactivity is measured. Rapidly changing metabolite concentrations in the blood can make the input function difficult to measure and compromise the application of a kinetic model, as was demonstrated with CGP 12177 (*19*). The observed metabolism of carazolol was minimal and was easily estimated. A balance occurred between the addition and removal of metabolites in the blood, resulting in an almost constant level throughout each study (Fig. 11). Carazolol activity in the plasma as a percentage of the total blood activity was relatively constant for both radiotracers throughout the study. This simple metabolic profile may allow studies to be performed with fewer metabolite analyses.

Among the ligands in its class of typical, sparingly metabolized, lipophilic, beta antagonists (*10–12*), carazolol is the only one which exhibits a useful degree of specific receptor binding in PET experiments. Another current ligand for PET imaging is [^{11}C]CGP 12177 (*19,20*), a similarly high-affinity, though hydrophilic, antagonist. It has been used to obtain quantitative estimations of receptors. Both tracers are considered to be nonspecific for beta receptor subtypes though only CGP 12177 is a partial agonist. Carazolol has a higher receptor affinity and is displaced from the receptors at about half the rate of CGP 12177, which may or may not provide modeling advantages. The initial uptake curves for both tracers have a similar shape and visualization of myocardium with both tracers is clear. The metabolism of CGP 12177 (*19*) was reported to be complete within minutes after injection. This caused any

estimation of the input function to be inaccurate and precluded application of the common kinetic models.

Though the high metabolic rate observed for the CGP compound may have been facilitated by its low lipophilicity, a comparison of these two compounds indicates that lipophilicity alone does not greatly affect overall receptor binding. The initial uptake in heart tissue, as a percent of injected dose, is similar for both compounds, though the fivefold higher specific activity of the carazolol used in this study caused accumulation of fewer picomoles of tracer per gram (1.0 vs. 4.0) in the heart than was published for CGP 12177 (*19*). The receptor-specific uptake ratio of both tracers is substantial, though a comparison cannot be made since this information was not published for CGP 12177. A new graphical approach to modeling was necessary to allow receptor estimation with CGP 12177. This approach involved assumptions specific to CGP 12177 and therefore could not be used to analyze carazolol data.

The main relative advantage of carazolol is that its metabolism is low and easily estimated. This should allow a conventional compartmental kinetic model to be applied to receptor analysis with carazolol. The relative lipophilicity of carazolol may also result in the ability to measure the total receptor population, including those which have been sequestered in short-term desensitization, and also may allow its application to beta-adrenergic receptors in the brain, though these possibilities have not yet been explored. These results lead us to expect that carazolol will be useful for receptor estimation and that it may present practical advantages in some clinical situations.

CONCLUSIONS

Both ^{11}C- and ^{18}F-labeled carazolols have been shown to give good quality PET images, a high degree of receptor-specific binding and low and predictable metabolite levels in the blood. The uptake curves in heart tissue are appropriate for application of kinetic modeling to determine receptor status. Nonspecific uptake was most easily and safely determined by use of the biologically less active enantiomer, R(+)-carazolol. These experiments indicate that it would be appropriate to continue by applying a kinetic receptor model to carazolol in the heart, to investigate its use in human subjects, and to investigate its receptor binding in the brain.

ACKNOWLEDGMENTS

The authors thank Ed Ellert and Laura Manfredi for their expert assistance with image analysis and Dr. Timothy Tewson for early discussions concerning the choice of ligand. This work was supported by the National Institutes of Health (HL43884).

REFERENCES

1. Sibley DR, Lefkowitz RJ. Molecular mechanisms of receptor desensitization using the β-adrenergic receptor-coupled adenylate cyclase system as a model. *Nature* 1985;317:124–129.
2. Lefkowitz RJ, Caron MG, Stiles GL. Mechanisms of membrane-receptor regulation. Biochemical, physiological and clinical insights derived from studies of the adrenergic receptors. In: Epstein FH, ed. *Mechanisms of disease. New Engl J Med* 1984;307:1570–1579.
3. Brodde O-E. β_1 and β_2-adrenoceptors in the human heart: properties, function, and alterations in chronic heart failure. *Pharmacol Rev* 1991;43:203–242.
4. Arango V, Ernsberger P, Marzuk PM, et al. Autoradiographic demonstration of increased serotonin 5-HT$_2$ and β-adrenergic receptor binding sites in the brain of suicide victims. *Arch Gen Psychiatry* 1990;47:1038–1047.
5. Berridge CW, Dunn AJ. Restraint-stress-induced changes in exploratory behavior appear to be mediated by norepinephrine-stimulated release of CRF. *J Neurosci* 1989;9:3513–3521.
6. Kalaria RN, Andorn AC, Tabaton M, Whitehouse PJ, Harik SI, Unnerstall JR. Adrenergic receptors in aging and Alzheimer's disease: increased β_2-receptors in prefrontal cortex and hippocampus. *J Neurochem* 1989;53:1772–1781.
7. Sisson JC, Wieland DM. Radiolabeled meta-iodobenzylguanidine: pharmacology and clinical studies. *Am J Physiol Imaging* 1986;1:96–103.
8. Glowniak JV, Turner FE, Gray LL, Palac RT, Lagunas-Solar MC, Woodward WR. Iodine-123-metaiodobenzylguanidine imaging of the heart in idiopathic congestive cardiomyopathy and cardiac transplants. *J Nucl Med* 1989;30:1182–1191.
9. Fagret D, Wolf J-E, Vanzetto G, Borrel E. Myocardial uptake of metaiodobenzylguanidine in patients with left ventricular hypertrophy secondary to valvular aortic stenosis. *J Nucl Med* 1993;34:57–60.
10. Berger G, Mazière M, Prenant C, Sastre J, Syrota A, Comar D. Synthesis of carbon-11-labeled propranolol. *J Radioanalyt Chem* 1982;74:301–304.
11. Berger G, Prenant C, Sastre J, Syrota A, Comar D. Synthesis of a β-blocker for heart visualization: [^{11}C]practolol. *Int J Appl Radiat Isot* 1983;34:1556–1557.
12. Prenant C, Sastre J, Crouzel C, Syrota A. Synthesis of [^{11}C]pindolol. *J Lab Cmpds Radiopharm* 1987;24:227–232.
13. Barovsky K, Brooker G. (−)-[^{125}I]-Iodopindolol, a new highly selective radioiodinated β-adrenergic receptor antagonist: measurement of β-receptors on intact rat astrocytoma cells. *J Cycl Nucl Res* 1980;6:297–307.
14. Tondo L, Conway PG, Brunswick DJ. Labeling in vivo of beta adrenergic receptors in the central nervous system of the rat after administration of [^{125}I]iodopindolol. *J Pharmacol Exp Therep* 1985;235:1–9.
15. Pazos A, Probst A, Palacios JM. β-adrenoceptor subtypes in the human brain: autoradiographic localization. *Brain Res* 1985;358:324–328.
16. Ezrailson EG, Garber AJ, Munson PJ, et al. [^{125}I]Iodocyanopindolol: a new β-adrenergic receptor probe. *J Cycl Nucl Res* 1981;7:13–26.
17. Buxton ILO, Brunton LL. Direct analysis of β-adrenergic receptor subtypes on intact adult ventricular myocytes of the rat. *Circ Res* 1985;56:126–132.
18. Francis B, Eckelman WC, Grissom MP, Gibson RE, Reba RC. The use of tritium labeled compounds to develop gamma-emitting receptor-binding radiotracers. *Int J Nucl Med Biol* 1982;9:173–179.
19. Delforge J, Syrota A, Lançon J-P, et al. Cardiac beta-adrenergic receptor density measured in vivo using PET, CGP 12177, and a new graphical method. *J Nucl Med* 1991;32:739–748.
20. Syrota A. Receptor binding studies of the living heart. *New Concepts Cardiac Imaging* 1988;4:141–166.
21. Conway PG, Tejani-Butt S, Brunswick DJ. Interaction of beta adrenergic agonists and antagonists with brain beta adrenergic receptors in vivo. *J Pharmacol Exp Ther* 1987;241:755–762.
22. Berridge MS, Cassidy EH, Terris AH, Vesselle J-M. Preparation and in vivo binding of [^{11}C]carazolol, a radiotracer for the beta-adrenergic receptor. *Nucl Med Biol* 1992;19:563–569.
23. Zheng L, Berridge MS, Ernsberger P. Synthesis, binding properties and ^{18}F labeling of flurocarazolol: a high affinity beta-adrenergic receptor antagonist. *J Med Chem* 1994: in press.
24. Berridge MS, Landmeier BJ. In-target production of [^{13}N]ammonia: target design, products, and operating parameters. *Int J Rad Appl Instrum [A]* 1993;44:1433–1441.
25. Nelson AD, Muzic RF, Miraldi F, Muswick GJ, Leisure GP, Voelker W. Continuous arterial positron monitor for quantitation in PET imaging. *Am J Physiol Imaging* 1990;5:84–88.
26. Nelson AD, Miraldi F, Muzic RF, Leisure GP, Semple WE. Noninvasive arterial monitor for quantitative $H_2{}^{15}O$ blood flow studies. *J Nucl Med* 1993;34:1000–1006.
27. Sorenson JA, Phelps ME. *Physics in nuclear medicine*. Orlando, FL: Grune and Stratton; 1987:254.
28. Farde L, Hall H, Ehrin E, Sedvall G. Quantitative analysis of D_2 dopamine receptor binding in the living human brain by PET. *Science* 1986;231:258–261.

29. Mintun MA, Raichle ME, Kilbourn MR, Wooten GF, Welch MJ. A quantitative model for the in vivo assessment of drug binding sites with positron emission tomography. *Ann Neurol* 1984;15:217–227.
30. Wong DF, Gjedde A, Wagner H. Quantification of neuroreceptors in the living human brain. I. Irreversible binding of ligands. *J Cereb Blood Flow Metab* 1986;6:137–146.
31. Manalan AD, Besch HR Jr, Watanabe AM. Characterization of [^{3}H]-(±)-carazolol binding to β-adrenergic receptors. Application to study of β-adrenergic receptor subtypes in canine ventricular myocardium and lung. *Circ Res* 1981;49:326–336.
32. Eckelman WC, ed. *Receptor-binding radiotracers*. Boca Raton: CRC Press; 1982:15–69.